



A data-driven topsoil $\delta^{13}\text{C}$ dataset and the drivers of spatial variability across the Tibetan Plateau

Yunsen Lai¹, Shaoda Li^{1, *}, Yuehong Shi¹, Xinrui Luo¹, Liang Liu¹, Peng Yu¹, Guo Chen², Longxi Cao², Chunju Cai³, Jian Sun⁴, Shaohui Chen⁵, Houyuan Lu^{6, 7, 8}, Xuanlong Ma⁹, Xiaolu Tang^{2, 10, *}

5 ¹ College of Earth Science, Chengdu University of Technology, Chengdu 610059, China

² College of Ecology and Environment, Chengdu University of Technology, Chengdu 610059, China

³ Key Laboratory of Bamboo and Rattan Science and Technology of National Forestry and Grassland Administration, International Centre for Bamboo and Rattan, Beijing 100102, China

10 ⁴ Key Laboratory of Alpine Ecology, Institute of Tibetan Plateau Research, Chinese Academy of Sciences, Beijing 100101, China

⁵ Key Laboratory of Water Cycle and Related Land Surface Processes, Institute of Geographic Sciences and Natural Resources Research, Chinese Academy of Sciences, Beijing 100101, China

⁶ Center for Excellence in Tibetan Plateau Earth Science, Chinese Academy of Sciences, Beijing 100101, China

⁷ University of Chinese Academy of Sciences, Beijing 100049, China

15 ⁸ Key Laboratory of Cenozoic Geology and Environment, Institute of Geology and Geophysics, Chinese Academy of Sciences, Beijing 100029, China

⁹ College of Earth and Environmental Sciences, Lanzhou University, Lanzhou 730000, China

¹⁰ State Environmental Protection Key Laboratory of Synergetic Control and Joint Remediation for Soil & Water Pollution, Chengdu University of Technology, Chengdu 610059, Chengdu, China

20 *Correspondence to:* Shaoda Li (1661348392@qq.com) and Xiaolu Tang (lxtt2010@163.com).

Abstract. Soil carbon isotopes ($\delta^{13}\text{C}$) provide reliable insights at a long-term scale for studying soil carbon turnover. The Tibetan Plateau (TP), called “the third pole of the earth” is one of the most sensitive areas to global climate change and exhibits an early warning signal of global warming. Although many studies detected the variability of soil $\delta^{13}\text{C}$ at site scales, a knowledge gap still exists in the spatial pattern of topsoil $\delta^{13}\text{C}$ across the TP. To fill the substantial knowledge gap, we first compiled a database of topsoil $\delta^{13}\text{C}$ with 396 observations from published literatures. Then we applied a Random Forest (RF) algorithm – a machine learning approach, to predict the spatial pattern of topsoil $\delta^{13}\text{C}$ and β (indicating the decomposition rate of soil organic carbon (SOC), calculated by $\delta^{13}\text{C}$ divided by logarithmically converted SOC). Finally, two datasets - topsoil $\delta^{13}\text{C}$ and β with a fine spatial resolution of 1 km across the TP were developed. Results showed that topsoil $\delta^{13}\text{C}$ varied significantly among different ecosystem types ($p < 0.001$). Topsoil $\delta^{13}\text{C}$ was -26.3 ± 1.60 ‰ (mean \pm standard deviation) for forests, 24.3 ± 2.00 ‰ for shrublands, -23.9 ± 1.84 ‰ for grasslands, -18.9 ± 2.37 ‰ for deserts, respectively. RF could well predict the spatial variability of topsoil $\delta^{13}\text{C}$ with a model efficiency of 0.62 and root mean square error of 1.12 ‰, enabling to derive data-driven $\delta^{13}\text{C}$ and β products. Data-driven topsoil $\delta^{13}\text{C}$ varied from -28.26 ‰ to -16.95 ‰,



with the highest topsoil $\delta^{13}\text{C}$ in the north and northwest TP and the lowest $\delta^{13}\text{C}$ in Southeast or South TP, indicating strong
35 spatial variabilities in topsoil $\delta^{13}\text{C}$. Similarly, there were strong spatial variabilities in data-driven β , with the lowest β values
at the east and middle TP, indicating a higher SOC turnover in the east and middle TP compared that of other regions in the
TP. This study was the first attempt to develop a fine resolution product of topsoil $\delta^{13}\text{C}$ and β across the TP, which could
provide an independent data-driven benchmark for biogeochemical cycling models to study SOC turnover and terrestrial
carbon-climate feedbacks over the TP under climate change. The data-driven $\delta^{13}\text{C}$ and β datasets are public available at
40 <https://doi.org/10.6084/m9.figshare.16641292.v2> (Tang, 2021)

1 Introduction

Soil organic carbon (SOC) is the largest carbon pool in terrestrial ecosystems, containing about 1500 Pg (1 Pg = 10^{15} g)
carbon within the first meter, which is two-fold higher than that of the atmosphere (Scharlemann et al., 2014). Due to the
decomposition of SOC, an amount of 57.2 Pg C was released from soil to the atmosphere (Tang et al., 2020). Thus a small
45 change in SOC could lead to a profound impact on the atmospheric CO_2 concentrations and hence climate change (Köchy et
al., 2015). Understanding SOC dynamics is of great importance to assess ecosystem carbon balance and its feedbacks to
climate change (Averill et al., 2014; Campbell et al., 2009; Wang et al., 2012). However, it is difficult to detect statistically
significant changes in soil carbon pool over a short time (Van Groenigen et al., 2014).

Carbon isotopes ($\delta^{13}\text{C}$) in soil organics provide reliable insights at the long-term scale into studying soil carbon turnover
50 (Acton et al., 2013; Blagodatskaya et al., 2011; Khan et al., 2008; Li et al., 2020). Because the majority of soil organic
matter originates from plant residues, soil $\delta^{13}\text{C}$ can well reflect vegetation-related soil formation and dynamics (Ehleringer et
al., 2000). Previous studies focused on spatial variability of soil $\delta^{13}\text{C}$ at in-site scale (Acton et al., 2013; Lu et al., 2004;
Wang et al., 2012). For example, it is widely observed that soil $\delta^{13}\text{C}$ values increase with the increasing soil depth and
increase with the decreasing soil organic carbon (Brunn et al., 2014; Wang et al., 2017; Wang et al., 2012). Climate, edaphic
55 variables, and their combinations have a vital influence on the spatial variability of soil $\delta^{13}\text{C}$ (Garten Jr et al., 2000).
However, modelling the spatial patterns of $\delta^{13}\text{C}$ using field observations has not been observed. A better understanding of
the spatial variability of soil $\delta^{13}\text{C}$ and its controlling factors at the regional scale is important to understand soil carbon
dynamics and potential feedbacks to climate change (Li et al., 2020; Rao et al., 2017; Zhao et al., 2019).

Previous studies found a negative linear correlation between the log-transformed SOC concentration and soil $\delta^{13}\text{C}$ (Acton
60 et al., 2013; Garten Jr and Hanson, 2006). The slope of the linear regression of soil $\delta^{13}\text{C}$ on log-transformed organic carbon
concentration is defined as β , a proxy of SOC decomposition (Garten Jr, 2006). The more negative the slope, the larger the
decrease in the β value and the faster the turnover rate (Campbell et al., 2009). The method was widely used to study SOC
turnover in the forest, grassland, and meadow ecosystems (Gautam et al., 2017; Peri et al., 2012; Zhao et al., 2019; Zhou et
al., 2019). Acton et al. (2013) noted that the β should be applied out in well-drained soils characterized by a gradual mixing



65 of litter and root carbon inputs decomposing in the soil profile. Empirical studies found that temperature, precipitation
(Acton et al., 2013), and soil properties (Wynn et al., 2006a) are important factors of driving β . However, temperature,
precipitation, and soil properties vary greatly with climate zones and biomes, indicating that there is a strong spatial pattern
of β . Therefore, detecting the spatial patterns of β is critical to study the SOC turnover to climate sensitivity. Whether β
values can be used to constrain rates and controls on SOC turnover has not been fully explored at regional scales,
70 particularly for areas with great sensitivity to climate change, e.g. the Tibetan Plateau (TP).

Due to highly data-adaptive and no initial assumptions on functional relationships between target variables and predict
variables, machine learning approaches, e.g. Random Forest (RF) (Breiman, 2001), have been widely applied in spatial
modelling in ecology and earth sciences using easy-to-measure variables (Tang et al., 2020; Yang et al., 2016). For example,
Tang et al. (2020) predicted soil heterotrophic respiration using RF and found that soil heterotrophic respiration increased
75 from 1980 to 2016 at the global scale. However, to date, no studies have used empirical field observations to assess the
spatial variability of soil $\delta^{13}\text{C}$ to bridge the knowledge gap between local, regional and global scales.

The TP is the largest and highest plateau with an average altitude of 4000 m above sea level and covers about 2.5×10^6
 km^2 on the earth (Lu et al., 2004). Soils in the TP store about 4.4 Pg (1 Pg = 10^{15} g) carbon within 30 cm (Yang et al., 2009),
accounting for 12.4% of total SOC in China's grasslands (Fang et al., 2010). In the last few decades, surface air temperature
80 in the TP has increased by 0.44 °C per decade, which was almost three times the world average (0.16 °C per decade) (Duan
and Xiao, 2015). Thus, it is urgent to explore the feedbacks between SOC and climate change under ongoing climate change.
Site-level studies found that the decomposition rate of SOC accelerates with temperature increase, resulting in the release of
stored carbon from the soil into the atmosphere (Chang et al., 2012; Dong et al., 2018; Li et al., 2020). However, regional
estimates of the sensitivity of SOC decomposition in the TP are still missing.

85 In this study, we firstly compiled a database of topsoil $\delta^{13}\text{C}$ from published literature based on field observations from
the TP and applied a Random Forest algorithm to predict the spatial patterns of topsoil $\delta^{13}\text{C}$ with the linkage of environment
variables. The objectives of this study are to: (1) compare the topsoil $\delta^{13}\text{C}$ among different ecosystems; (2) develop gridded
products of topsoil $\delta^{13}\text{C}$ and β (named data-driven $\delta^{13}\text{C}$ and β); (3) explore the spatial pattern of topsoil $\delta^{13}\text{C}$ and β over the
TP. The outcome can provide an insightful view of the SOC dynamics and turnover across the TP.

90 2 Materials and methods

2.1 Data sources

The first topsoil (0 – 5 cm) $\delta^{13}\text{C}$ dataset based on field observations was from Lu et al. (2004) and second dataset was
Qi (2017). Along different elevation gradients, soil samples were collected away from the villages and leaves, grass roots,
and litter were removed before sampling (Lu et al., 2004; Qi, 2017). Finally, a total of 396 observations were included in the
95 study, with 16 observations from deserts, 103 observations from forests, 218 observations from grasslands and 59
observations from shrublands. Meanwhile, site information, included altitude, vegetation type, latitude and longitude, was
also included.

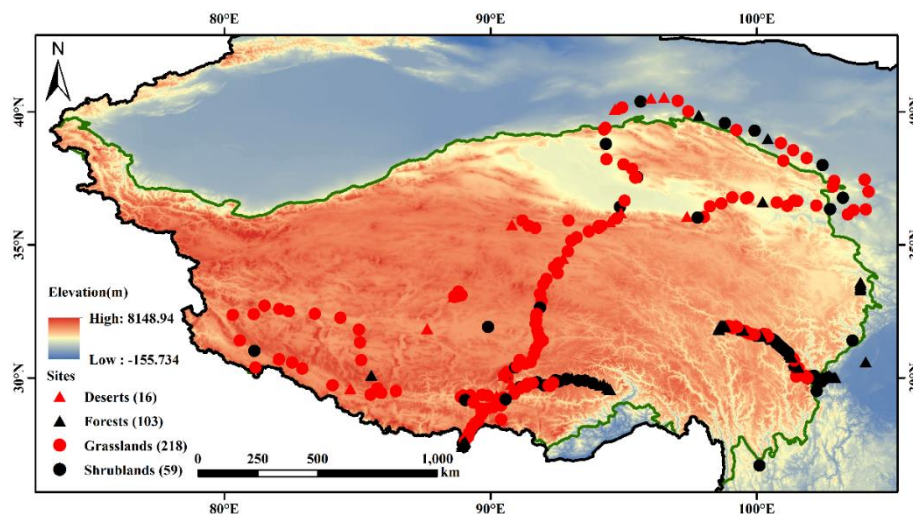


Figure 1. The distributions of the study sites.

100 2.2 Environmental variables

Topsoil $\delta^{13}\text{C}$ is affected by multiple environmental factors. To investigate the spatial patterns of $\delta^{13}\text{C}$, the spatial grid of environmental variables was required. The environmental variables were included: mean annual temperature (MAT) and mean annual precipitation (MAP) with the spatial resolution is 1 km during 2000-2010 from Peng et al. (2019). The elevation data (digital elevation map; DEM) with 1 km spatial resolution was obtained from National Earth System Science Data Center (<http://www.geodata.cn>). Moderate-resolution Imaging Spectroradiometer (MODIS) products, including normalized difference vegetation index (NDVI) and enhanced vegetation index (EVI) with a spatial resolution of 1 km, leaf area index (LAI) and the fraction of photosynthetically active radiation (FPAR), with a spatial resolution of 500 m, gross primary productivity (GPP) with a spatial resolution of 500 m, evapotranspiration (ET) and potential evapotranspiration (PET) with a spatial resolution of 500 m, land cover type (LCT), with a spatial resolution of 500 m were from <https://lpdaac.usgs.gov/>.
105
110 Due to data availability, NDVI, EVI and GPP covered from 2000 to 2010, while ET and PET covered from 2001 to 2010, and LAI and FPAR covered from 2002 to 2010. The soil organic content, soil pH, soil BD, soil silt content, soil clay content, soil sand content with 250 m spatial resolution were from SoilGrids (Hengl et al., 2017). Before data analysis, the soil and MODIS data were resampled to 1 km using the nearest neighbour method.

2.3 Data analysis

115 One-way analysis of variance (ANOVA) was performed to analyse the significance difference in topsoil $\delta^{13}\text{C}$ among forests, shrublands, grasslands and deserts. If the difference was significant at the 0.05 level, the Tukey-HSD (honestly significant difference) test was applied for multiple comparisons. Tukey-HSD is a post-hoc test based on the studentized range distribution that determines which specific groups' means are different by comparing all possible pairs of means



(Bretz et al., 2016). The correlation analysis was conducted to explore the correlations between topsoil $\delta^{13}\text{C}$ and climate,
120 vegetations and soil factors.

The β values, which reflect the sensitivity of SOC decomposition (Garten Jr, 2006), were obtained using a standard least-squares regression analysis between the log10-transformed SOC concentration and $\delta^{13}\text{C}$:

$$\delta^{13}\text{C}_{\text{SOC}} = \beta \times \lg(\text{SOC}) + \alpha \quad (1)$$

Where $\delta^{13}\text{C}_{\text{SOC}}$ is the $\delta^{13}\text{C}$ in SOC, and the β value is the regression coefficient. The α value is a constant number, which
125 was obtained using a standard-least squares regression analysis between the log10-transformed SOC concentration and soil $\delta^{13}\text{C}$ from gathering dataset (Fig. S1). In current study, the spatial resolution 250 m SOC within 0 – 5 cm from SoilGrids was used (Hengl et al., 2017). All the analyses were conducted in R 3.6.3 (R Core Team, 2018).

2.4 Spatial modelling

2.4.1 Feature selection

130 In order to improve the model efficiency and reduce the workload, a recursive feature elimination (RFE) algorithm was used for variable selection (Kuhn, 2008). RFE improves the generalization efficiency by avoiding overfitting while reducing the complexity of the model. In general, RFE is to select features by recursively considering smaller and smaller feature sets: first, all input variables participate in random forest modelling and rank the importance of participating variables; second, a new feature set is obtained by removing the corresponding proportion of unimportant indicators from the current feature
135 variables; third, a new random forest is created with the new feature set, and the variable importance of each feature in the feature set is calculated and ranked. The three steps are repeated until best features remained. Finally, six variables (MAT, MAP, Altitude, NDVI, Vegetation types, pH) were selected to predict topsoil $\delta^{13}\text{C}$. Figure S1 shows that the relative importance evaluation of all the variables.

2.4.2 Modelling

140 RF was used to model the spatial patterns of topsoil $\delta^{13}\text{C}$. RF is an ensemble machine learning algorithm that predicts a response from a set of predictors by creating multiple decision trees and aggregating their results (Breiman, 2001). RF algorithm has two important custom parameters, the number of categorical regression trees and the number of random variables separating the nodes. Model prediction accuracy can be improved by optimizing these two parameters (Liaw and Wiener, 2002). However, RF models are usually insensitive to the number of trees or variables. RF regression can handle a
145 large number of features and aids feature selection according to the importance value of each variable for avoiding overfitting (Bodesheim et al., 2018; Jian et al., 2018; Tang et al., 2020). In the present study, the RF model was trained by *caret* package (version 6.0-80) by linking *RandomForest* in R, and then the model was implemented to predict topsoil $\delta^{13}\text{C}$ for each grid with a spatial resolution of 1 km. To evaluate the performance of RF, a 10-fold cross-validation was applied, which meant that the data set was stratified into 10 parts, and each part contained approximately an equal number of samples. The



150 target values for each of these ten parts were predicted using a model trained using the remaining nine parts (Jung et al.,
2011; Tang et al., 2020). The model efficiency (R^2) and root-mean-square error (RMSE) were used to model evaluation
(Tang et al., 2020; Yao et al., 2018).

3. Results

3.1 Soil $\delta^{13}\text{C}$ among different ecosystems

155 Large variabilities of soil $\delta^{13}\text{C}$ values were observed among different ecosystem types (Fig. 2 and Table S1). $\delta^{13}\text{C}$ ranges
from -29.71‰ in forests to -15.08‰ in deserts, and mean $\delta^{13}\text{C}$ was $-24.41 \pm 2.38\text{‰}$ (mean \pm standard deviation). In terms
of ecosystem types, $\delta^{13}\text{C}$ varied significantly (Fig. 2, $p < 0.001$), specifically, the highest $\delta^{13}\text{C}$ was $-18.9 \pm 2.37\text{‰}$ in deserts,
followed by grasslands ($-23.9 \pm 1.84\text{‰}$) and shrublands ($-24.3 \pm 2.00\text{‰}$), forests with the lowest $\delta^{13}\text{C}$ ($-26.3 \pm 1.60\text{‰}$,
Table S1). There was no difference in soil $\delta^{13}\text{C}$ between grasslands and shrublands ($p = 0.423$). Great variability was also
160 observed within the same ecosystem type. For example, topsoil $\delta^{13}\text{C}$ varied from -28.8‰ to -18.2‰ in shrublands.

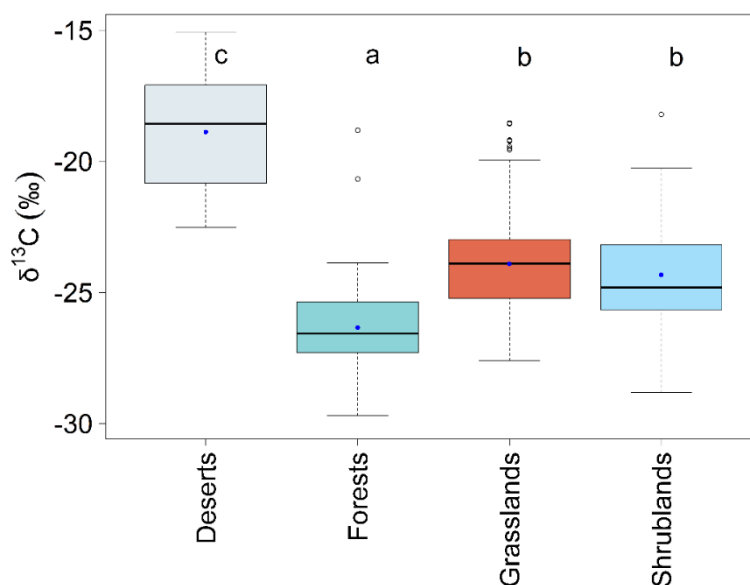
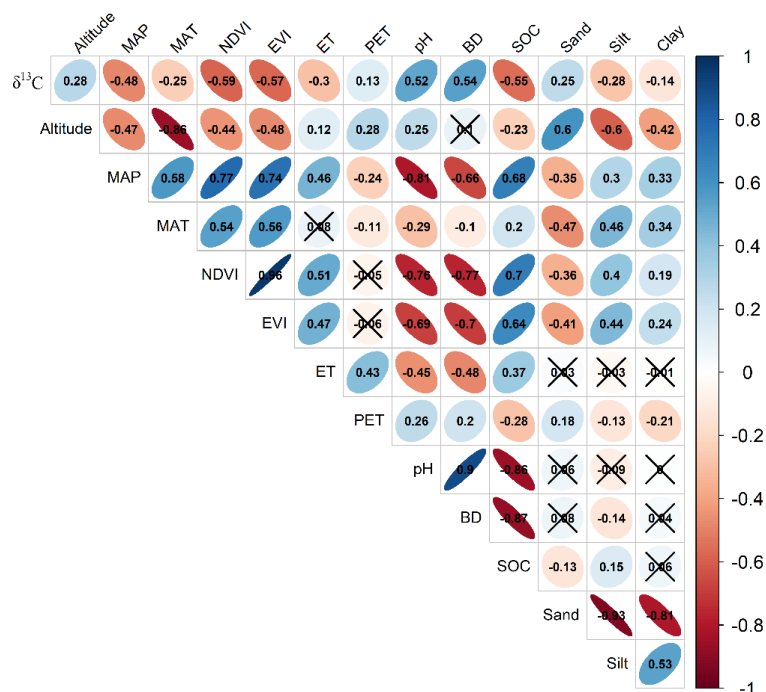


Figure 2. Boxplot of topsoil $\delta^{13}\text{C}$ among different ecosystem types. The boxplot shows the median (line), first and third
quartiles (box bounds), 1.5 times the interquartile (whiskers) and outliers (values outside of whisker limits) for each
ecosystem type. Different lowercase letters (a, b and c) indicate significantly different ratios at $p < 0.05$ using one-way
165 analysis of variance (ANOVA) and Tukey-HSD test for multiple comparisons. The blue dots represent the mean topsoil $\delta^{13}\text{C}$.

3.2 Relationships between soil $\delta^{13}\text{C}$ and environmental factors



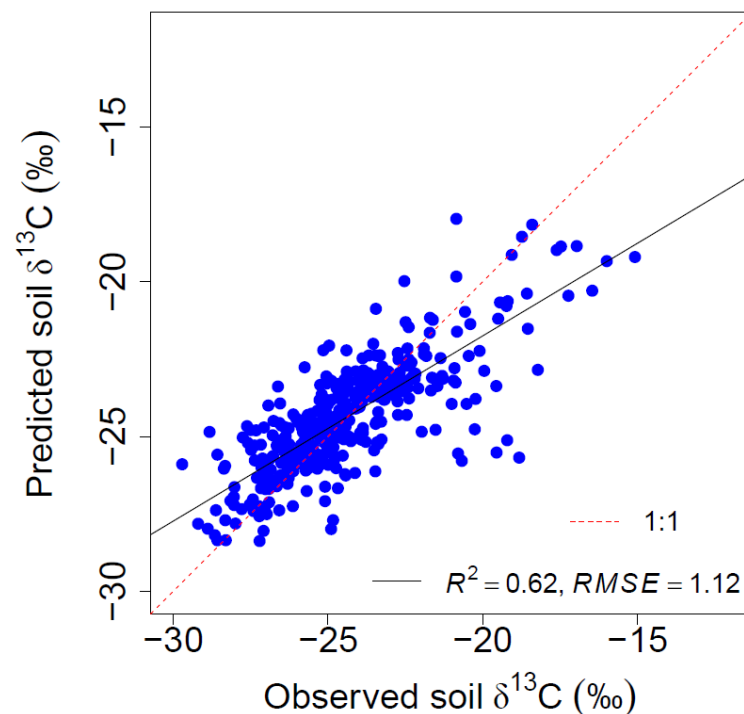
170 Climate, soil and vegetation variables led to a significant impact on soil $\delta^{13}\text{C}$. Positive correlations were found between soil $\delta^{13}\text{C}$ and altitude, PET, pH, BD and soil sand content, while negative correlations were found between soil $\delta^{13}\text{C}$ and MAP, MAT, NDVI, EVI, ET, SOC, soil clay and silt content (Fig. 3).



175 **Figure 3.** The correlation coefficient analysed by the Pearson correlation between soil $\delta^{13}\text{C}$ and environmental factors. The numbers marked by “x” means insignificance at the level of $p < 0.05$. MAT: mean annual temperature ($^{\circ}\text{C}$); MAP: mean annual precipitation (mm); ET: evapotranspiration (kg m^{-2}); PET: potential evapotranspiration (kg m^{-2}); NDVI: normalized difference vegetation index; Altitude: elevation (m); BD: soil bulk density (g cm^{-3}); SOC: soil organic carbon content (g kg^{-1}); pH: soil pH; Sand: soil sand content (%); Clay: soil clay content (%); Silt: soil silt content (%).

3.3 Spatial patterns of the data-driven $\delta^{13}\text{C}$

Based on the 10-fold cross-validation, R^2 and RMSE were 0.62 and 1.12 %, respectively, indicating that RF can well predict the spatial patterns of topsoil $\delta^{13}\text{C}$ (Fig. 4).



180

Figure 4. Correlations between observed and predicted soil $\delta^{13}\text{C}$ from Random Forest by 10-fold cross-validation.

The data-driven $\delta^{13}\text{C}$ showed great spatial variation across the TP. The highest topsoil $\delta^{13}\text{C}$ was observed in the north and northwest TP, while the lowest topsoil $\delta^{13}\text{C}$ was in Southeast or South TP. Across the TP, soil $\delta^{13}\text{C}$ varied from -28.26 ‰ to -16.95 ‰, and mean topsoil $\delta^{13}\text{C}$ was -22.26 ‰.

185

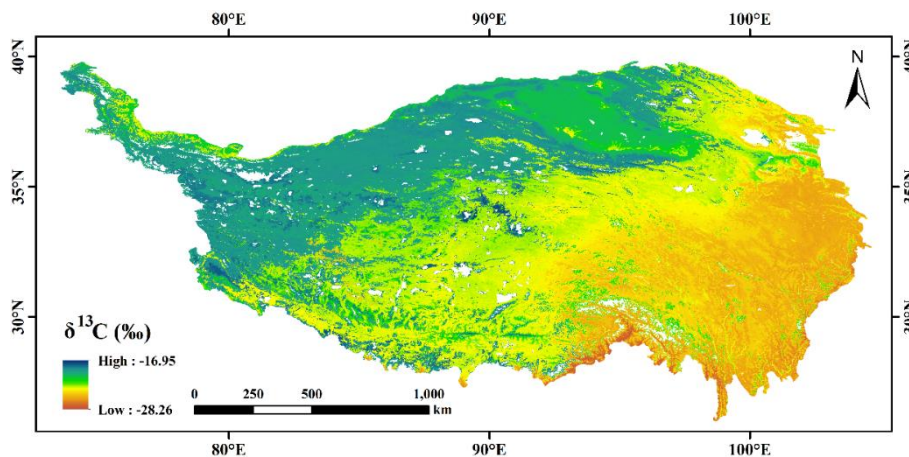


Figure 5. Spatial distributions of the data-driven $\delta^{13}\text{C}$ of topsoil across the TP.



3.4 Spatial variability of the data-driven β across the TP

The data-driven β also showed strong spatial variabilities across the TP (Fig. 6). The highest β values were found in northwest and north regions, while the lowest values were observed in the middle-west TP with β lower than -8. Mean β was -2.33 across the TP.

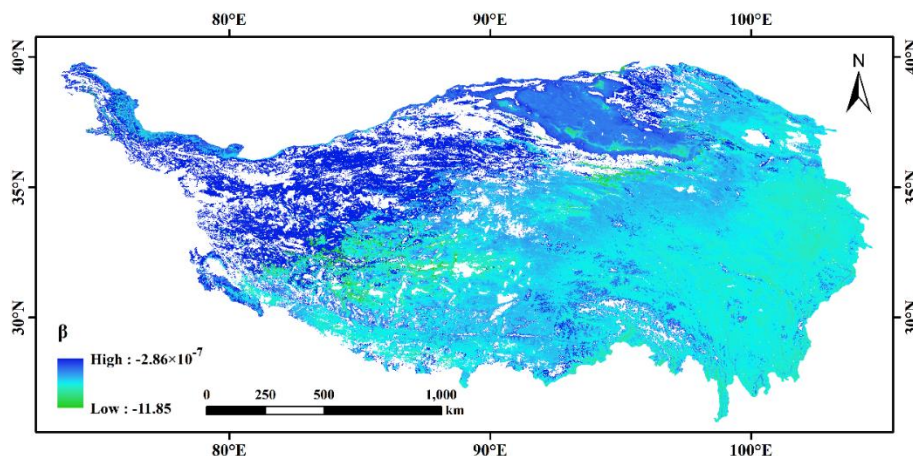


Figure 6. Spatial distributions of the data-driven β of topsoil across the TP.

4 Discussion

195 4.1 Spatial variations of the data-driven $\delta^{13}\text{C}$ across the TP

We found significant differences in topsoil $\delta^{13}\text{C}$ across ecosystems, with an increasing trend from forests (-26.3 ‰), shrublands (-24.3 ‰), grasslands (-23.9 ‰) to deserts (-18.9 ‰) (Table S1). The result was similar to previous study (Wang et al., 2012), which found that topsoil $\delta^{13}\text{C}$ was -25.25‰ for forests, -24.71‰ for meadow and -23.65‰ for steppe.

For the first time, we developed a data-driven $\delta^{13}\text{C}$ of topsoil using RF, and found a great spatial pattern in topsoil $\delta^{13}\text{C}$, with an increasing trend from the southeast to the northwest TP. Such spatial patterns may be primarily associated with vegetation types (Wang et al., 2012), because we found that vegetation types was the most important factor in predicting topsoil $\delta^{13}\text{C}$ (Fig. S2). Plant litter was the main source of soil organic matter and plant litter production varied greatly among different ecosystem types. Therefore, different vegetation types with large differences in leaf $\delta^{13}\text{C}$ could lead to a significant impact on topsoil $\delta^{13}\text{C}$ (Wang et al., 2012; Yang et al., 2015). Plant species growing in dry habitats generally have high leaf $\delta^{13}\text{C}$ values (Wang et al., 2012). For example, C_4 plants, growing in the high elevation of the TP with a strong ability to adapt to severe drought, had much higher leaf $\delta^{13}\text{C}$ than C_3 plants (Wang et al., 2004). Meanwhile, the degree of carbon isotope fractionation during the conversion of soil organic matter from different regions and plant residues varied, ranging from 0.5 ‰ to 2 ‰ (Cao et al., 2005). The southeast TP was dominated by forests, and the northwest TP was dominated by



deserts and grasslands (Wang et al., 2012), which could potentially lead to higher soil $\delta^{13}\text{C}$ in the northwest TP and lower
210 soil $\delta^{13}\text{C}$ in the southeast TP (Fig. 4).

Besides vegetation types, climate factors were also important to influence the spatial variation of topsoil $\delta^{13}\text{C}$ (Wang et al., 2013; Rao et al., 2012; Zhao et al., 2017). The data-driven $\delta^{13}\text{C}$ had a significant and negative correlation with MAT (Fig. 3), indicating that temperature could lead to a significant impact on topsoil $\delta^{13}\text{C}$. Our results were consistent with Rao et al. (2017) and Zhang et al. (2020), who found topsoil $\delta^{13}\text{C}$ decreased with the increase of MAT. However, the data-driven $\delta^{13}\text{C}$
215 were different from Wang et al. (2012) and Zhang et al. (2020), and they found a positive correlation between topsoil $\delta^{13}\text{C}$ and MAT. The controversial results may be associated with the relative complexity between temperature and topsoil $\delta^{13}\text{C}$ (Rao et al., 2017). First, the temperature can affect topsoil $\delta^{13}\text{C}$ by changing $\delta^{13}\text{C}$ in vegetation and microbial characteristics. For example, temperature could affect the relative abundance of C_3 and C_4 plants (Tieszen et al., 1997). Generally, a relatively higher abundance of C_4 plants distribution was found in higher MAT and lower MAP areas (Zhang et al., 2003).
220 Second, temperature could also affect carbon isotope fractionation by modulating the stomatal conductance of plants and the activities of photosynthetic enzymes (Rao et al., 2017; Zhao et al., 2017). With the increase of temperature, plants close to the leaf stomata decrease the intercellular CO_2 , thus leading to the increase of $\delta^{13}\text{C}$ in plants. Third, temperature could also affect topsoil $\delta^{13}\text{C}$ by regulating the decomposition rate of litter and ecosystem respiration (Cai et al., 2021; Kato et al., 2004). Generally, a lower temperature led to a lower litter decomposition and ecosystem respiration, enriching soil $\delta^{13}\text{C}$.
225 Fourth, the temperature can also affect topsoil $\delta^{13}\text{C}$ by changing isotopic fractionation during the microbial decomposition (Garten Jr, 2006). Microbes tend to use lighter ^{12}C during the decomposition and ^{13}C component accumulates. Therefore, the combined effects of lower stomatal conductance and lower enzyme activity resulted in a negative correlation between topsoil $\delta^{13}\text{C}$ and temperature (Li et al., 2020; Zhang et al., 2020), and higher topsoil $\delta^{13}\text{C}$ in north and northwest TP (Fig. 4).

Precipitation is another important factor influencing soil $\delta^{13}\text{C}$. Our results showed that topsoil $\delta^{13}\text{C}$ decreases with
230 increasing precipitation (Fig. 3), which was consistent with previous studies (Murphy and Bowman, 2009; Zhao et al., 2019). The mechanisms of the impact of precipitation on $\delta^{13}\text{C}$ have been well explained. It is generally accepted that because of the lack of water, vegetation will close stomata to reduce transpiration, leading to an increase in $\delta^{13}\text{C}$ (Farquhar et al., 1989). In the last several decades, the TP suffered from a significant increase in MAT and MAP, which may increase the species, microbial quantities and activities (Papatheodorou et al., 2004), accelerating the decomposition rate of ^{12}C , enriching soil
235 $\delta^{13}\text{C}$ (Li et al., 2020). In the north TP, precipitation was much lower than in the south TP (Fig. S3). Therefore, the change of vegetation types, the closure of stomata due to the lack of precipitation and the increase microbial activities due to increasing MAT and MAP may partly explain the higher topsoil $\delta^{13}\text{C}$ in the north TP compared to other regions of the TP.

Soil factors may influence soil $\delta^{13}\text{C}$ by altering microbial activity, matrix quality, and effectiveness (Wynn et al., 2006b; Xu et al., 2016). Generally, soil $\delta^{13}\text{C}$ decreased with the increase of SOC (Wang et al., 2018; Yang et al., 2015), and
240 increased with the increase of soil sand content (Wang et al., 2012). This is consistent with our study that we found a negative correlation between the data-driven $\delta^{13}\text{C}$ and SOC, and a positive correlation between the data-driven $\delta^{13}\text{C}$ and sand



content (Fig. 3). Meanwhile, soil texture can lead to a significant impact on SOC dynamics and affect soil $\delta^{13}\text{C}$ (Bird et al., 2002). Soil $\delta^{13}\text{C}$ increases with decreasing particle size because carbon enriched in $\delta^{13}\text{C}$ is allocated to microbial biomass and can subsequently be stabilized by the interaction with soil fine mineral phases (Kleber et al., 2011; Sollins et al., 2009).
245 We found that topsoil $\delta^{13}\text{C}$ was negatively correlated with soil silt content (Fig. 3). This result is consistent with the study from Wang et al. (2012) in the TP.

4.2 Spatial patterns of the data-driven β across the TP

Soil carbon turnover is a major determinant of the capacity of soil carbon sequestration (Luo et al., 2003), and a decrease in carbon turnover can sequester SOC without an increase in carbon input (Jastrow et al., 2006). Because it is
250 difficult to detect the change in SOC stock over short periods due to the large pool size and huge spatial heterogeneity (Van Groenigen et al., 2014), the predicted β across the TP could provide a reliable method to evaluate the SOC turnover rate over a large spatial scale (Brunn et al., 2014; Gautam et al., 2017). Therefore, understanding the spatial variation of the β values is particularly important.

The β values reflect the turnover rate of SOC in response to microbial activities. The more negative the β values and the
255 faster turnover of SOC (Acton et al., 2013; Zhao et al., 2019). Although many studies have compared β values among different ecosystem types across the TP and suggested that β was a useful proxy for understanding generalized patterns of SOC turnover and the underlying control over soil metabolism (Wang et al., 2018), knowledge gaps still exist in the spatial variability of β . This study was the first time to estimate the spatial patterns of β across the TP, which could improve our understanding of the spatial patterns of SOC turnover and contribute to predicting the soil C dynamics and feedback of soil C
260 cycle to climate change. There was a great spatial pattern of the data-driven β across the TP, highlighting the large variability in SOC turnover. The lowest β values were below -10, locating at the east and middle TP, which was much lower than the observed β values ranging from -0.60 to -7.41 (Wang et al., 2018; Zhao et al., 2019), indicating that SOC turnover was faster in the east and middle TP compared that of other regions and highlighting the need of protecting SOC in the TP under the ongoing climate change.

Understanding how the environmental variables that affects the spatial patterns of β values is a key goal for
265 understanding the SOC dynamics. The temperature and precipitation are important variables that have the significant effect on SOC turnover (Li et al., 2020; Wang et al., 2017). Generally, increasing temperature and precipitation can stimulate the turnover rate of SOC by affecting the soil microbial biomass and enzyme activities (Collins et al., 2008; Conant et al., 2011), and vice versa. Our study found that β values were low in the east TP and high in the north and northwest TP, indicating that
270 SOC turnover rate in the east TP was faster than that in the north and northwest TP. This result may result from differences in climate because MAT and MAP in the north or northwest TP were much lower compared to the east TP (Fig. S3 and Fig. S4). Our result also agreed with a previous study that the SOC turnover increased with increasing temperature at a global scale (Wang et al., 2018).



Besides climate, soil properties also lead to a significant impact on SOC turnover. A previous study indicated that β values were generally negatively correlated with sand content and positively correlated with clay content in the TP (Li et al., 2020). Our results generally agreed with the previous study that β values were high in the northwest TP where soil sand content was low, and soil clay content was high (Fig. S5 and Fig. S6). It is widely accepted that soil texture could affect SOC turnover by changing soil water-holding capacity, water movement, gas diffusion (Kaiser et al., 2015; Yiqi and Zhou, 2010; Xu et al., 2016). Meanwhile, soil pH can also affect SOC turnover by altering microbial community and enzyme activity, along with substrate availability (Priha et al., 2001). Therefore, the spatial patterns of β values were jointly controlled by climate and soil properties, and detecting the dominant environmental control on β values can enhance the predictive power for addressing the spatial patterns of SOC turnover, as well as for understanding the future response of SOC to climate change.

4.3 Limitations

In this study, based on the topsoil $\delta^{13}\text{C}$ field observations dataset, we developed a data-driven $\delta^{13}\text{C}$ of topsoil using a RF algorithm and analysed its spatial pattern across the TP, however, limitations still remain in a few aspects. First, the RF algorithm builds a model based on the training dataset, which is usually limited by data in terms of quantity, quality, and representativeness. In many ecological studies around the world, uneven data distribution has always been a well-known problem (e.g., Jung et al. (2011) and Xu and Shang (2016)). The study sites of topsoil $\delta^{13}\text{C}$ were mainly concentrated in the eastern and northern TP, while there were a lack of topsoil $\delta^{13}\text{C}$ field observations in the western and northwest TP. Therefore, the uneven coverage of observations was an important source of uncertainty to predict topsoil $\delta^{13}\text{C}$, which may cause a bias in the RF model towards the areas with more observations. In the future studies, increasing the number of field observations in the eastern and northern TP could improve the ability to evaluate spatial pattern of topsoil $\delta^{13}\text{C}$ across the TP. Second, our dataset was from the topsoil within 0 – 5 cm, although it is generally accepted that topsoil generally had higher carbon content and more sensitive to environmental change compared to subsoils. Therefore, modelling soil $\delta^{13}\text{C}$ for deeper soils would greatly improve our understanding of soil carbon dynamics and its response to carbon-climate feedbacks across the TP.

5 Data availability

There were three datasets in our study. The first dataset was topsoil $\delta^{13}\text{C}$ from field observations. The second and third datasets were data-driven $\delta^{13}\text{C}$ and β with a spatial resolution of 1 km using RF algorithm. The datasets were publicly available for scientific purposes and freely downloaded at <https://doi.org/10.6084/m9.figshare.16641292.v2> (Tang, 2021).

6 Conclusions

Gridded data-driven $\delta^{13}\text{C}$ and β of topsoil with a spatial resolution of 1 km were developed based on field observations using RF. Our results showed that topsoil $\delta^{13}\text{C}$ varied significantly among ecosystem types, indicating that vegetation types



305 led to a significant impact on topsoil $\delta^{13}\text{C}$. Data-driven $\delta^{13}\text{C}$ of topsoil varied from -28.29 ‰ to -16.95 ‰ and $\delta^{13}\text{C}$ was increasing from southeast to northwest. Similarly, strong spatial variabilities were observed in data-driven β and increased from eastern to northwest, indicating that SOC turnover was higher in the east TP compared to that of the northwest TP. The data-driven $\delta^{13}\text{C}$ and β of topsoil could provide an independent benchmark for biogeochemical models to study SOC turnover and terrestrial carbon-climate feedbacks under ongoing climate change in the TP.

310
Competing interests. The authors declare that they have no conflict of interest.

Author contribution. YL, SL and XT design the study; YS, XL, LL and PY contributed to data analysis, including proving R code; GC and LC provided constructive comments. Other authors contributed to review the manuscript.

315
Acknowledgement. The authors express their great thanks Houyuan Lu and Lin Qi for contribution of field data collection. Great thanks also to the data providers – MODIS team, climate data from Peng et al. (2019) and soil data from (Hengl et al., 2017), etc.

320 **Financial support.** This study was primarily supported by the Everest Scientific Research Program, Chengdu University of Technology (80000-2021ZF11410), Sichuan Science and Technology Program (2019YFG0460, 2021YJ0377), Fundamental Research Funds for Platform of International Centre for Bamboo and Rattan (1632020003); Operation Funding of Innovation Platform of Forest and Grass Technology (2021132033, 2021132035), State Key Laboratory of Geohazard Prevention and Geoenvironment Protection Independent Research Project (SKLGP2018Z004, SKLGP2021K024).

325 **References**

- Acton, P., Fox, J., Campbell, E., Rowe, H., and Wilkinson, M.: Carbon isotopes for estimating soil decomposition and physical mixing in well-drained forest soils, *J Geophys Res-Biogeophys*, 118, 1532-1545, <https://doi.org/10.1002/2013jg002400>, 2013.
- Averill, C., Turner, B. L., and Finzi, A. C.: Mycorrhiza-mediated competition between plants and decomposers drives soil carbon storage, *Nature*, 505, 543-545, <https://doi.org/10.1038/nature12901>, 2014.
- 330 Bird, M. I., Santrůcková, H., Lloyd, J., and Lawson, E.: The isotopic composition of soil organic carbon on a north–south transect in western Canada, *Eur. J. Soil Sci.*, 53, 393-403, <https://doi.org/10.1046/j.1365-2389.2002>.
- Blagodatskaya, E., Yuyukina, T., Blagodatsky, S., and Kuzyakov, Y.: Turnover of soil organic matter and of microbial biomass under C3-C4 vegetation change: Consideration of ^{13}C fractionation and preferential substrate utilization, *Soil Biol. Biochem.*, 43, 159-166, <https://doi.org/10.1016/j.soilbio.2010.09.028>, 2011.
- 335 Bodesheim, P., Jung, M., Gans, F., Mahecha, M. D., and Reichstein, M.: Upscaled diurnal cycles of land-atmosphere fluxes: a new global half-hourly data product, *Earth Syst Sci Data*, 10, 1-47, <https://doi.org/10.5194/essd-10-1327-2018>, 2018.
- Breiman, L. J. M. L.: *Random Forests*, *Mach Learn*, 45, 5-32, <https://doi.org/10.1023/A:1010933404324>, 2001.
- Bretz, F., Hothorn, T., and Westfall, P.: *Multiple comparisons using R*, Chapman and Hall/CRC 2016.
- 340 Brunn, M., Spielvogel, S., Sauer, T., and Oelmann, Y.: Temperature and precipitation effects on $\delta^{13}\text{C}$ depth profiles in SOM under temperate beech forests, *Geoderma*, 235-236, 146-153, <https://doi.org/10.1016/j.geoderma.2014.07.007>, 2014.
- Cai, A. D., Liang, G. P., Yang, W., Zhu, J., Han, T. F., Zhang, W. J., and Xu, M. G.: Patterns and driving factors of litter



- decomposition across Chinese terrestrial ecosystems, *J Clean Prod*, 278, 123964, <https://doi.org/10.1016/j.jclepro.2020.123964>, 2021.
- 345 Campbell, J. E., Fox, J. F., Davis, C. M., Rowe, H. D., and Thompson, N.: Carbon and Nitrogen Isotopic Measurements from Southern Appalachian Soils: Assessing Soil Carbon Sequestration under Climate and Land-Use Variation, *J. Environ. Eng.*, 135, 439-448, [https://doi.org/10.1061/\(ASCE\)Ec.1943-7870.0000008](https://doi.org/10.1061/(ASCE)Ec.1943-7870.0000008), 2009.
- Cao, Y., Liu, W., Ning, Y., Zhang, Q., and Wang, Z.: Effects of soil sample preparation process on $\delta^{13}\text{C}$ of organic matter, *Geochemistry*, 34, 91-100 (in Chinese), 2005.
- 350 Chang, X., Wang, S., Luo, C., Zhang, Z., Duan, J., Zhu, X., Lin, Q., and Xu, B.: Responses of soil microbial respiration to thermal stress in alpine steppe on the Tibetan plateau, *Eur. J. Soil Sci.*, 63, 325-331, <https://doi.org/10.1111/j.1365-2389.2012.01441.x>, 2012.
- Collins, S. L., Sinsabaugh, R. L., Crenshaw, C., Green, L., Porras-Alfaro, A., Stursova, M., and Zeglin, L. H.: Pulse dynamics and microbial processes in aridland ecosystems, *J. Ecol.*, 96, 413-420, <https://doi.org/10.1111/j.1365-2745.2008.01362.x>, 2008.
- 355 Conant, R. T., Ryan, M. G., Ågren, G. I., Birge, H. E., Davidson, E. A., Eliasson, P. E., Evans, S. E., Frey, S. D., Giardina, C. P., Hopkins, F. M., Hyvönen, R., Kirschbaum, M. U. F., Lavelle, J. M., Leifeld, J., Parton, W. J., Megan Steinweg, J., Wallenstein, M. D., Martin Wetterstedt, J. Å., and Bradford, M. A.: Temperature and soil organic matter decomposition rates - synthesis of current knowledge and a way forward, *Global Change Biol.*, 17, 3392-3404, <https://doi.org/10.1111/j.1365-2486.2011.02496.x>, 2011.
- 360 Dong, S., Li, Y., Zhao, Z., Li, Y., Liu, S., Zhou, H., Dong, Q., Li, S., Gao, X., and Shen, H.: Land Degradation Enriches Soil $\delta^{13}\text{C}$ in Alpine Steppe and Soil $\delta^{15}\text{N}$ in Alpine Desert by Changing Plant and Soil Features on Qinghai-Tibetan Plateau, *Soil Sci. Soc. Am. J.*, 82, 960-968, <https://doi.org/10.2136/sssaj2018.01.0017>, 2018.
- Duan, A. and Xiao, Z. J. S. R.: Does the climate warming hiatus exist over the Tibetan Plateau, *Scientific Reports*, 5, 1-9, <https://doi.org/10.1038/srep13711>, 2015.
- 365 Ehleringer, J. R., Buchmann, N., and Flanagan, L. B.: Carbon isotope ratios in belowground carbon cycle processes, *Ecol. Appl.*, 10, 412-422, <https://doi.org/10.1890/1051-0761>, 2000.
- Fang, J., Yang, Y., Ma, W., Mohammad, A., and Shen, H.: Ecosystem carbon stocks and their changes in China's grasslands, *Science China. Life sciences*, 53, 757-765, <https://doi.org/10.1007/s11427-010-4029-x>, 2010.
- 370 Farquhar, G. D., Ehleringer, J. R., and Hubick, K. T.: Carbon isotope discrimination and photosynthesis, *Annual review of plant biology*, 40, 503-537, <https://doi.org/10.1146/annurev.pp.40.060189.002443>, 1989.
- Garten Jr, C. T.: Relationships among forest soil C isotopic composition, partitioning, and turnover times, *Canadian Journal of Forest Research*, 36, 2157-2167, <https://doi.org/10.1139/X06-115>, 2006.
- Garten Jr, C. T. and Hanson, P. J.: Measured forest soil C stocks and estimated turnover times along an elevation gradient, *Geoderma*, 136, 342-352, <https://doi.org/10.1016/j.geoderma.2006.03.049>, 2006.
- 375 Garten Jr, C. T., Cooper, L. W., Post III, W., and Hanson, P. J.: Climate controls on forest soil C isotope ratios in the southern Appalachian Mountains, *Ecology*, 81, 1108-1119, <https://doi.org/10.1890/0012-9658>, 2000.
- Gautam, M. K., Lee, K.-S., Song, B.-Y., and Bong, Y.-S.: Site related $\delta^{13}\text{C}$ of vegetation and soil organic carbon in a cool temperate region, *Plant Soil*, 418, 293-306, <https://doi.org/10.1007/s11104-017-3284-z>, 2017.
- 380 Hengl, T., Mendes de Jesus, J., Heuvelink, G. B., Ruiperez Gonzalez, M., Kilibarda, M., Blagotic, A., Shangguan, W., Wright, M. N., Geng, X., Bauer-Marschallinger, B., Guevara, M. A., Vargas, R., MacMillan, R. A., Batjes, N. H., Leenaars, J. G., Ribeiro, E., Wheeler, I., Mantel, S., and Kempen, B.: SoilGrids250m: Global gridded soil information based on machine learning, *PLoS One*, 12, e0169748, <https://doi.org/10.1371/journal.pone.0169748>, 2017.
- Jastrow, J. D., Amonette, J. E., and Bailey, V. L.: Mechanisms controlling soil carbon turnover and their potential application for enhancing carbon sequestration, *Clim. Change*, 80, 5-23, <https://doi.org/10.1007/s10584-006-9178-3>, 2006.
- 385 Jian, J., Steele, M. K., Thomas, Q., Day, S. D., and Hodges, S. C. J. G. C. B.: Constraining estimates of global soil respiration by quantifying sources of variability, *Glob Chang Biol*, 24, 4143-4159, <https://doi.org/10.1111/gcb.14301>, 2018.
- Jung, M., Reichstein, M., Margolis, H. A., Cescatti, A., Richardson, A. D., Arain, M. A., Arneth, A., Bernhofer, C., Bonal, D., and Chen, J.: Global patterns of land-atmosphere fluxes of carbon dioxide, latent heat, and sensible heat derived from eddy covariance, satellite, and meteorological observations, *J Geophys Res-Biogeophys*, 116, <https://doi.org/10.1029/2010JG001566>, 2011.
- 390 Kaiser, M., Kleber, M., and Berhe, A. A.: How air-drying and rewetting modify soil organic matter characteristics: An



- assessment to improve data interpretation and inference, *Soil Biol. Biochem.*, 80, 324-340, <https://doi.org/10.1016/j.soilbio.2014.10.018>, 2015.
- 395 Kato, T., Tang, Y., Gu, S., Cui, X., Hirota, M., Du, M., Li, Y., Zhao, X., and Oikawa, T.: Carbon dioxide exchange between the atmosphere and an alpine meadow ecosystem on the Qinghai–Tibetan Plateau, China, *Agricultural forest meteorology*, 124, 121-134, <https://doi.org/10.1016/j.agrformet.2003.12.008>, 2004.
- Khan, K. S., Gattinger, A., Buegger, F., Schloter, M., and Joergensen, R. G.: Microbial use of organic amendments in saline soils monitored by changes in the $^{13}\text{C}/^{12}\text{C}$ ratio, *Soil Biol. Biochem.*, 40, 1217-1224, <https://doi.org/10.1016/j.soilbio.2007.12.016>, 2008.
- 400 Kleber, M., Nico, P. S., Plante, A., Filley, T., Kramer, M., Swanston, C., and Sollins, P.: Old and stable soil organic matter is not necessarily chemically recalcitrant: implications for modeling concepts and temperature sensitivity, *Global Change Biol.*, 17, 1097-1107, <https://doi.org/10.1111/j.1365-2486.2010.02278.x>, 2011.
- Köchy, M., Hiederer, R., and Freibauer, A.: Global distribution of soil organic carbon – Part 1: Masses and frequency distributions of SOC stocks for the tropics, permafrost regions, wetlands, and the world, *Soil*, 1, 351-365, <https://doi.org/http://dx.doi.org/10.5194/soil-1-351-2015>, 2015.
- 405 Kuhn, M.: Building predictive models in R using the caret package, *Journal of statistical software*, 28, 1-26, 2008.
- Li, H., Yan, F., Tuo, D., Yao, B., and Chen, J.: The effect of climatic and edaphic factors on soil organic carbon turnover in hummocks based on $\delta^{13}\text{C}$ on the Qinghai-Tibet Plateau, *Sci. Total Environ.*, 741, 140141, <https://doi.org/10.1016/j.scitotenv.2020.140141>, 2020.
- 410 Liaw, A. and Wiener, M. J. R. n.: Classification and regression by randomForest, 2, 18-22, 2002.
- Lu, H. Y., Wu, N. Q., Gu, Z. Y., Guo, Z. T., Wang, L., Wu, H. B., Wang, G., Zhou, L. P., Han, J. M., and Liu, T. S.: Distribution of carbon isotope composition of modern soils on the Qinghai-Tibetan Plateau, *Biogeochemistry*, 70, 273-297, <https://doi.org/10.1023/B: BIOG.0000049343.48087.ac>, 2004.
- 415 Luo, Y., White, L. W., Canadell, J. G., DeLucia, E. H., Ellsworth, D. S., Finzi, A., Lichter, J., and Schlesinger, W. H.: Sustainability of terrestrial carbon sequestration: A case study in Duke Forest with inversion approach, *Global biogeochemical cycles*, 17, <https://doi.org/10.1029/2002GB001923>, 2003.
- Murphy, B. P. and Bowman, D. M. J. S.: The carbon and nitrogen isotope composition of Australian grasses in relation to climate, *Funct. Ecol.*, 23, 1040-1049, <https://doi.org/10.1111/j.1365-2435.2009.01576.x>, 2009.
- 420 Papatheodorou, E. M., Argyropoulou, M. D., and Stamou, G. P.: The effects of large- and small-scale differences in soil temperature and moisture on bacterial functional diversity and the community of bacterivorous nematodes, *Applied Soil Ecology*, 25, 37-49, [https://doi.org/10.1016/S0929-1393\(03\)00100-8](https://doi.org/10.1016/S0929-1393(03)00100-8), 2004.
- Peng, S. Z., Ding, Y. X., Liu, W. Z., and Li, Z.: 1 km monthly temperature and precipitation dataset for China from 1901 to 2017, *Earth System Science Data*, 11, 1931-1946, <https://doi.org/10.5194/essd-11-1931-2019>, 2019.
- 425 Peri, P. L., Ladd, B., Pepper, D. A., Bonser, S. P., Laffan, S. W., and Amelung, W.: Carbon ($\delta^{13}\text{C}$) and nitrogen ($\delta^{15}\text{N}$) stable isotope composition in plant and soil in S outhern P atagonia's native forests, *Global Change Biol.*, 18, 311-321, <https://doi.org/10.1111/j.1365-2486.2011.02494.x>, 2012.
- Priha, O., Grayston, S. J., Hiukka, R., Pennanen, T., and Smolander, A.: Microbial community structure and characteristics of the organic matter in soils under *Pinus sylvestris*, *Picea abies* and *Betula pendula* at two forest sites, *Biol. Fertility Soils*, 33, 17-24, <https://doi.org/DOI 10.1007/s003740000281>, 2001.
- 430 Qi, L.: Distribution of Organic Carbon Isotope Composition for Modern Soils from the Eastern Margin of the Tibetan Plateau and its Main Controlling Factors, Doctor, China University of Geosciences, Wuhan., 2017.
- R Core Team: R: A language and environment for statistical computing, R Foundation for Statistical Computing Vienna, Austria, available at: <http://www.R-project.org/> (last access: 11 March 2019), 2018.
- 435 Rao, Z., Chen, F., Zhang, X., Xu, Y., Xue, Q., and Zhang, P.: Spatial and temporal variations of C₃/C₄ relative abundance in global terrestrial ecosystem since the Last Glacial and its possible driving mechanisms, *Chin. Sci. Bull.*, 57, 4024-4035, <https://doi.org/10.1007/s11434-012-5233-9>, 2012.
- Rao, Z., Guo, W., Cao, J., Shi, F., Jiang, H., and Li, C.: Relationship between the stable carbon isotopic composition of modern plants and surface soils and climate: A global review, *Earth-Sci. Rev.*, 165, 110-119, <https://doi.org/10.1016/j.earscirev.2016.12.007>, 2017.
- 440 Scharlemann, J. P. W., Tanner, E. V. J., Hiederer, R., and Kapos, V.: Global soil carbon: understanding and managing the largest terrestrial carbon pool, *Carbon Management*, 5, 81-91, <https://doi.org/10.4155/Cmt.13.77>, 2014.



- Sollins, P., Kramer, M. G., Swanston, C., Lajtha, K., Filley, T., Aufdenkampe, A. K., Wagai, R., and Bowden, R. D.: Sequential density fractionation across soils of contrasting mineralogy: evidence for both microbial- and mineral-controlled soil organic matter stabilization, *Biogeochemistry*, 96, 209-231, <https://doi.org/10.1007/s10533-009-9359-z>, 2009.
- 445 Tang, X.: A data-driven estimate of topsoil (0-5 cm) isotope carbon across the Tibetan Plateau, 10.6084/m9.figshare.16641292.v2, 2021.
- Tang, X., Fan, S., Du, M., Zhang, W., Gao, S., Liu, S., Chen, G., Yu, Z., and Yang, W.: Spatial and temporal patterns of global soil heterotrophic respiration in terrestrial ecosystems, *Earth Syst. Sci. Data*, 12, 1037-1051, <https://doi.org/10.5194/essd-12-1037-2020>, 2020.
- 450 Tieszen, L. L., Reed, B. C., Bliss, N. B., Wylie, B. K., and Dejong, D. D.: NDVI characteristics, potential C3 and C4 grass production, and delta-13C values in grassland land cover classes of the Great Plains, *Ecol. Appl.*, 7, 59-78, <https://doi.org/10.1890/1051-0761>, 1997.
- Van Groenigen, K. J., Qi, X., Osenberg, C. W., Luo, Y., and Hungate, B. A.: Faster decomposition under increased atmospheric CO2 limits soil carbon storage, *Science*, 344, 508-509, <https://doi.org/10.1126/science.1249534>, 2014.
- 455 Wang, Luo, Lu, Houyuan, Wu, Naiqin, Chu, Duo, Han, and Jiamao: Discovery of C4 species at high altitude in Qinghai-Tibetan Plateau, *Chinese Science Bulletin*, 49, 1392-1396, <https://doi.org/10.1007/BF03036887>, 2004.
- Wang, C., Houlton, B. Z., Liu, D., Hou, J., Cheng, W., and Bai, E.: Stable isotopic constraints on global soil organic carbon turnover, *Biogeosciences*, 15, 987-995, <https://doi.org/10.5194/bg-15-987-2018>, 2018.
- 460 Wang, C., Wei, H., Liu, D., Luo, W., Hou, J., Cheng, W., Han, X., and Bai, E.: Depth profiles of soil carbon isotopes along a semi-arid grassland transect in northern China, *Plant Soil*, 417, 43-52, <https://doi.org/10.1007/s11104-017-3233-x>, 2017.
- Wang, G. A., Li, J. Z., Liu, X. Z., and Li, X. Y.: Variations in carbon isotope ratios of plants across a temperature gradient along the 400 mm isohaline of mean annual precipitation in north China and their relevance to paleovegetation reconstruction, *Quaternary Science Reviews*, 63, 83-90, <https://doi.org/10.1016/j.quascirev.2012.12.004>, 2013.
- 465 Wang, S., Fan, J., Song, M., Yu, G., Zhou, L., Liu, J., Zhong, H., Gao, L., Hu, Z., Wu, W., and Song, T.: Patterns of SOC and soil 13C and their relations to climatic factors and soil characteristics on the Qinghai-Tibetan Plateau, *Plant Soil*, 363, 243-255, <https://doi.org/10.1007/s11104-012-1304-6>, 2012.
- Wynn, J. G., Harden, J. W., and Fries, T. L.: Stable carbon isotope depth profiles and soil organic carbon dynamics in the lower Mississippi Basin, *Geoderma*, 131, 89-109, <https://doi.org/10.1016/j.geoderma.2005.03.005>, 2006a.
- 470 Wynn, J. G., Bird, M. I., Vellen, L., Grand-Clement, E., Carter, J., and Berry, S. L.: Continental-scale measurement of the soil organic carbon pool with climatic, edaphic, and biotic controls, *Global Biogeochem. Cycles*, 20, n/a-n/a, <https://doi.org/10.1029/2005gb002576>, 2006b.
- Xu, M. and Shang, H.: Contribution of soil respiration to the global carbon equation, *J Plant Physiol*, 203, 16-28, <https://doi.org/10.1016/j.jplph.2016.08.007>, 2016.
- 475 Xu, X., Shi, Z., Li, D., Rey, A., Ruan, H., Craine, J. M., Liang, J., Zhou, J., and Luo, Y.: Soil properties control decomposition of soil organic carbon: Results from data-assimilation analysis, *Geoderma*, 262, 235-242, <https://doi.org/10.1016/j.geoderma.2015.08.038>, 2016.
- Yang, R.-M., Zhang, G.-L., Liu, F., Lu, Y.-Y., Yang, F., Yang, F., Yang, M., Zhao, Y.-G., and Li, D.-C.: Comparison of boosted regression tree and random forest models for mapping topsoil organic carbon concentration in an alpine ecosystem, *Ecol. Indicators*, 60, 870-878, <https://doi.org/10.1016/j.ecolind.2015.08.036>, 2016.
- 480 Yang, Y., Ji, C., Chen, L., Ding, J., Cheng, X., Robinson, D., and Whitehead, D.: Edaphic rather than climatic controls over 13C enrichment between soil and vegetation in alpine grasslands on the Tibetan Plateau, *Funct. Ecol.*, 29, 839-848, <https://doi.org/10.1111/1365-2435.12393>, 2015.
- Yang, Y., Fang, J., Smith, P., Tang, Y., Chen, A., Ji, C., Hu, H., Rao, S., Tan, K., and HE, J. S.: Changes in topsoil carbon stock in the Tibetan grasslands between the 1980s and 2004, *Global Change Biology*, 15, 2723-2729, <https://doi.org/10.1111/j.1365-2486.2009.01924.x>, 2009.
- 485 Yao, Y., Wang, X., Li, Y., Wang, T., Shen, M., Du, M., He, H., Li, Y., Luo, W., and Ma, M. J. G. c. b.: Spatiotemporal pattern of gross primary productivity and its covariation with climate in China over the last thirty years, *Glob Chang Biol*, 24, 184-196, <https://doi.org/10.1111/gcb.13830>, 2018.
- 490 Yiqi, L. and Zhou, X.: Soil respiration and the environment, Elsevier 2010.
- Zhang, D., Yang, Y., and Ran, M.: Variations of surface soil $\delta^{13}\text{C}_{\text{org}}$ in the different climatic regions of China and paleoclimatic implication, *Quaternary International*, 536, 92-102, <https://doi.org/10.1016/j.quaint.2019.12.015>, 2020.



- 495 Zhang, Z., Zhao, M., Lu, H., and Faiia, A. M.: Lower temperature as the main cause of C4 plant declines during the glacial periods on the Chinese Loess Plateau, *Earth Planetary Science Letters*, 214, 467-481, [https://doi.org/10.1016/S0012-821X\(03\)00387-X](https://doi.org/10.1016/S0012-821X(03)00387-X), 2003.
- Zhao, Y., Wu, F., Fang, X., and Yang, Y.: Altitudinal variations in the bulk organic carbon isotopic composition of topsoil in the Qilian Mountains area, NE Tibetan Plateau, and its environmental significance, *Quaternary International*, 454, 45-55, <https://doi.org/10.1016/j.quaint.2017.08.045>, 2017.
- 500 Zhao, Y., Wang, X., Ou, Y., Jia, H., Li, J., Shi, C., and Liu, Y.: Variations in soil $\delta^{13}\text{C}$ with alpine meadow degradation on the eastern Qinghai–Tibet Plateau, *Geoderma*, 338, 178-186, <https://doi.org/10.1016/j.geoderma.2018.12.005>, 2019.
- Zhou, Y., Zhang, W., Cheng, X., Harris, W., Schaeffer, S. M., Xu, X., and Zhao, B.: Factors affecting ^{13}C enrichment of vegetation and soil in temperate grasslands in Inner Mongolia, China, *J. Soils Sed.*, 19, 2190-2199, <https://doi.org/10.1007/s11368-019-02248-z>, 2019.

505